Journal Pre-proofs

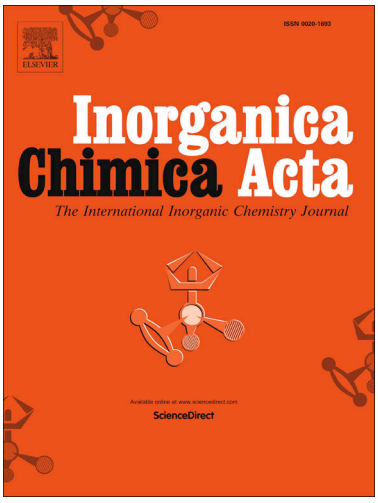

Synthesis of a tetratopic bisphosphine ligand derived from pyrimidine and its incorporation into gold and silver coordination polymers

Roberta R. Rodrigues, Eric W. Reinheimer, Christopher L. Dorsey, Todd W. Hudnall

PII: S0020-1693(22)00421-2
DOI: https://doi.org/10.1016/j.ica.2022.121209
Reference: ICA 121209

To appear in: *Inorganica Chimica Acta*

Received Date: 19 July 2022
Revised Date: 9 September 2022
Accepted Date: 16 September 2022

Please cite this article as: R.R. Rodrigues, E.W. Reinheimer, C.L. Dorsey, T.W. Hudnall, Synthesis of a tetratopic bisphosphine ligand derived from pyrimidine and its incorporation into gold and silver coordination polymers, *Inorganica Chimica Acta* (2022), doi: https://doi.org/10.1016/j.ica.2022.121209

Synthesis of a tetratopic bisphosphine ligand derived from pyrimidine and its incorporation into gold and silver coordination polymers.

Roberta R. Rodrigues,[1†] Eric W. Reinheimer,[2] Christopher L. Dorsey,[1] and Todd W. Hudnall[1,*]

1. Department of Chemistry and Biochemistry, Texas State University, 601 University Drive, San Marcos, TX, 78666, USA

2. Rigaku Americas Corporation, 9009 New Trails Dr, The Woodlands, TX 77381, USA.

KEYWORDS Multitopic ligands, bisphosphine, bisphosphonium, coordination polymer.

ABSTRACT: Herein we present the synthesis of a tetratopic bisphosphine ligand derived from 4,6-disubstituted pyrimidine scaffold. This new ligand (**2**) was doubly alkylated using iodomethane to give bisphosphonium dication (**3**) as an iodide salt, and was also coordinated to both gold(I) chloride to give the metal complex (**4**) and to silver(I) triflate to give a coordination polymer (**5**), respectively. All compounds have been fully characterized using multinuclear NMR spectroscopy as well as single crystal X-ray diffraction. Gold complex **4** was also found to exhibit weak emission at λ_{max} = 530 nm due to Au(I)–Au(I) aurophilic interactions. Additionally we demonstrated that bisphosphine ligand **2** can be used as a tetratopic ligand, as evidenced by the formation of the coordination polymer **5** in which both phosphine→silver and nitrogen→silver interactions were observed.

1. Introduction

The development of multitopic ligands continues to be a major research thrust globally.[1-6] While there are several categories of multitopic ligands available to the synthetic chemist, those containing multiple phosphorus or nitrogen[3] donor sites, and more recently, multitopic carbenes,[7, 8] have perhaps received the most attention. Such ligands, especially those containing two or more phosphine ligands such as JOSIPHOS[9] (Figure 1), have enjoyed a rich and continuing history in the areas of catalysis,[10, 11] coordination chemistry,[6, 12, 13] molecular recognition,[2] organometallic chemotherapeutics,[14, 15] and as building blocks in MOFs[5] and COFs as well as ligands in luminescent materials.[4] Indeed, homogenous, organocatalysis, and more recently, photoredox catalysis[16, 17] are all underpinned by the use of phosphine ligands.

In the realm of multitopic ligands, the so-called pincer ligands featuring diphosphino and/or triphosphino[18] ligands have been explored by several groups. A random selection of the vast assortment of homogeneous catalysts featuring some common pincer ligand motifs such as PNP,[19] PCP,[20] PPP,[21] and PONOP[22] arrangements are provided in Figure 1. Additionally, Peters,[23] Gabbaï,[24, 25] and Ozerov[26, 27] have independently utilized diphosphine-containing pincer ligands to stabilize main group element/transition metal complexes for applications in photoreductive elimination/redox-noninnocent catalysts and homogeneous catalysis, respectively. (Figure 1).

In recent years, phosphine and the heavier arsine ligands have been incorporated into MOFs. In this area, Wade[28] and Humphrey[29] have successfully prepared immobilized

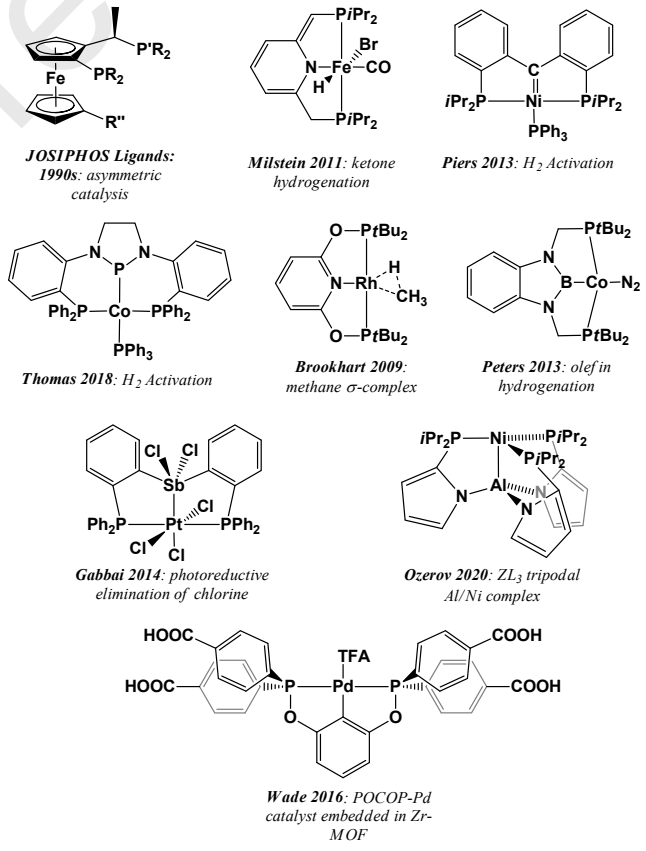

Figure 1. Examples of the utility of multitopic diphosphine ligands in synthesis and catalysis.

catalysts and uniquely confined Au_2Cl_2, which exhibited enhanced catalytic activity and exceptionally short aurophilic interactions, respectively. Indeed, Wade demonstrated that the Zr-MOF supported POCOP-Pd(II) catalysts was a highly active transfer hydrogenation catalyst, when in contrast, a homogenous variant was found to decompose under similar experimental conditions.

For the past decade, our research group has been investigating the synthesis and reactivity of exceptionally π-acidic carbene ligands. In an effort to prepare pincer-type multitopic π-acidic carbenes featuring phosphino groups, we became interested in utilizing 4,6-dichloropyrimidine, **1**, as a commercially available starting material. While we have been unsuccessful in preparing multitopic carbene ligands to date using compound **1**, we have had some success in introducing diphenylphosphino moieties into the 4- and 6-positions of the pyrimidine scaffold to afford the tetratopic bisphosphinopyrimidine, **2**.[30, 31] Herein we report a new synthesis, characterization, and coordination chemistry of compound **2**.

2. Experimental

2.1 General considerations

Unless noted otherwise, all procedures were carried out using standard Schlenk techniques under an atmosphere of dry nitrogen or in a nitrogen-filled glove box. Solvents were dried and degassed by an Innovative Technology solvent purification system and stored over 3 Å molecular sieves in a nitrogen-filled glovebox. 1,4-dioxane, dichloromethane-D2 (CD_2Cl_2), chloroform-D (CDCl3), and acetonitrile-D3 (CD_3CN) were dried over 3 Å molecular sieves and distilled. Potassium diphenylphosphide ($KPPh_2$) and (tht)gold(I)chloride were prepared according to literature procedures. [32, 33] Diphenylphosphine (Ph_2PH) was purchased from Alfa Aesar, and 4,6-dichloropyrimidine (1) was purchased from Matrix scientific; both were used as without purification. Potassium hydride was purchased as a 30% w/w suspension in mineral oil from Thermo Scientific. It was transferred into the glove box, poured into a sintered glass frit funnel and washed with hexanes to remove the mineral oil. All other reagents and solvents were used as received. Elemental analyses were performed at Midwest Microlabs, LLC (Indianapolis, IN). Fluorescence spectra were obtained on a BioTek Synergy H4 hybrid microplate reader equipped with a Take3 cuvette holder accessory.

2.2 Synthesis of compounds **2**–**5**

Starting from commercially available **1**, all compounds were prepared in good to excellent yields according to the scheme described in Scheme 1 below.

Synthesis of **2**: Inside of a nitrogen-filled glove box, a 100 mL Schlenk flask was charged with **1** (0.500 g, 3.36 mmol), potassium diphenylphosphide (1.66 g, 7.39 mmol), and THF (50 mL). The flask was sealed and removed from the glove box, whereupon it was stirred overnight at ambient temperature. After that time, all volatiles were removed from the yellow suspension. The residue was dissolved in dichloromethane (50 mL) and then filtered over a one-inch plug of silica topped with Celite. The solvent was then removed *in vacuo* to afford compound **2** as a white crystalline solid, 0.830 g, 1.85 mmol (55%, yield). ^{1}H NMR ($CDCl_3$): δ 6.69 (s, 1H),

Scheme 1: Synthesis of compounds **2**-**5**.

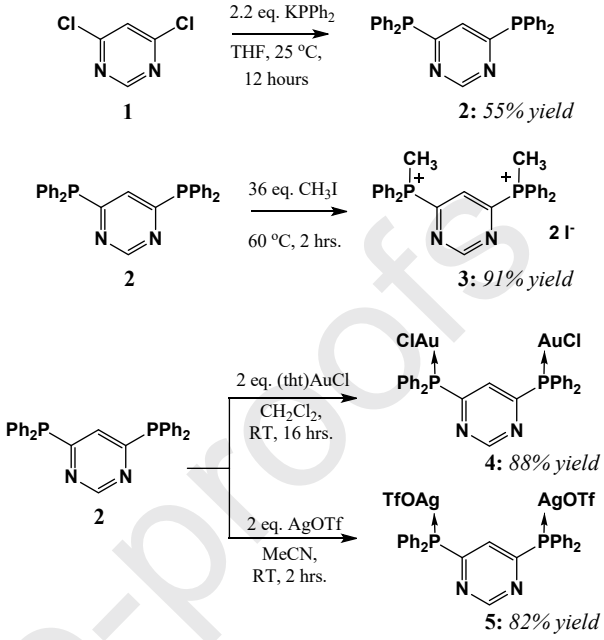

7.31-7.33 (m, 20H, P*Ph*), 9.20 (s, 1H). ^{13}C NMR ($CDCl_3$): δ 126.76 (t, $^2J_{C\text{-}P}$ = 12.2 Hz, pyrimidine - *C5*), 128.78 (d, $J_{C\text{-}P}$ = 7.96 Hz, Ph*C*), 129.62 (s, Ph*C*), 133.60 (d, $^1J_{C\text{-}P}$ = 8.9 Hz, *ipso*-Ph*C*), 134.28 (d, $J_{C\text{-}P}$ = 20.5 Hz, Ph*C*), 156.83 (t, $J_{C\text{-}P}$ = 9.45 Hz, pyrimidine - *C4*/*C6*), 174.26 (d, $J_{C\text{-}P}$ = 7.00 Hz, pyrimidine – *C2*). ^{31}P NMR ($CDCl_3$): δ -3.12.

Synthesis of **3**: A 5 mL thick-walled pressure tube equipped with a Teflon screw cap was charged with **2** (100 mg, 0.223 mmol) and a magnetic stirring bar. To the flask 0.5 mL of iodomethane (1.14 g, 8.03 mmol) was then added. The reaction tube was closed and the mixture was heated to 60 °C for 2 hours. After that time, the bright red-orange solution was cooled to room temperature, and then diethyl ether (10 mL) was added. The reaction tube was again sealed and the suspension was sonicated in an ultrasonic bath for 30 minutes to induce precipitation of the product as an orange solid. The compound was isolated by filtration and dried in vacuo to give 149 mg, 0.205 mmol (91% yield) of 3 as an orange solid. ^{1}H NMR ($CDCl_3$): δ 3.42 (d, $^2J_{H\text{-}P}$ = 13.92 Hz, 6H, P-C*H*$_3$), 7.57-7.61 (m, 8H, P*Ph*), 7.69-7.71 (m, 4H, P*Ph*), 8.07-8.12 (m, 8H, P*Ph*), 9.03 (m, 1H), 9.56 (s, 1H). ^{13}C NMR ($CDCl_3$/CD_3CN): δ 8.40 (d, $^1J_{C\text{-}P}$ = 55.1 Hz, *ipso*-Ph*C*), 129.71 (t, $J_{C\text{-}P}$ = 6.87 Hz, Ph*C*), 131.10 (t, $J_{C\text{-}P}$ = 5.47 Hz, Ph*C*), 135.10 (s, Ph*C*), 156.18 (d, $^1J_{C\text{-}P}$ = 6.36 Hz, pyrimidine - *C5*), 157.08 (d, $J_{C\text{-}P}$ = 6.44 Hz, pyrimidine – *C2*), 158.25 (t, $J_{C\text{-}P}$ = 16.37 Hz, pyrimidine - *C4*/*C6*). ^{31}P NMR ($CDCl_3$): δ 19.30.

Synthesis of **4**: Inside of a nitrogen-filled glovebox, a 10 mL Schlenk flask was charged with 100 mg (0.223 mmol) of compound **2**, and 144 mg (0.446 mmol) of (tht)AuCl. To the solids was added dichloromethane (5 mL). The flask was sealed, removed from the glovebox, and the reaction mixture

was stirred at ambient temperature for 16 hours. After this time, all volatiles were removed in vacuo, then the residue was washed with diethyl ether (5 x 5 mL). The solid was then dried to give 182 mg (0.194 mmol) of compound **4** as a white solid (87.5% yield). ^{1}H NMR (CD_2Cl_2): δ 7.48-7.51 (m, 9H, P*Ph*), 7.58-7.62 (m, 4H, P*Ph*), 7.66-7.69 (m, 8H, P*Ph*), 9.42 (s, 1H). ^{13}C NMR (CD_2Cl_2): δ 125.96 (d, $^{1}J_{C-P}$ = 63.5 Hz, *ipso*-PhC), 129.71-130.06 (m, PhC), 133.32 (s, PhC), 135.18-135.29 (m, PhC), 159.17 (t, $^{1}J_{C-P}$ = 14.04 Hz, pyrimidine - *C5*), 166.43 (d, J_{C-P} = 4.69 Hz, pyrimidine – *C4*/*C6*), 167.03 (d, J_{C-P} = 4.71 Hz, pyrimidine – *C2*). ^{31}P NMR (CD_2Cl_2): δ 33.33.

Synthesis of **5**: Inside of a nitrogen-filled glovebox, a 25 mL Schlenk flask was charged with 100 mg (0.223 mmol) of compound **2** and 114 mg (0.446 mmol) of AgOTf. Then 10 mL of acetonitrile was added and the reaction was allowed to stir at room temperature for 12 hours. After that time, the solvent was reduced to approximately 3 mL then diethyl ether (20 mL) was added which induced precipitation of the product as an off white solid. The product was isolated by filtration, washed with ether, then dried *in vacuo* to give 175 mg (0.182 mmol) of compound **5** as an off-white solid (82 % yield). Despite repeated washings with diethyl ether and drying *in vacuo*, residual acetonitrile (~ 2 equivalents) could not be removed for NMR analysis. ^{1}H NMR (CD_3CN): δ 2.23 (s, 5H, CH_3CN), 6.32 (s, 1H), 7.41-7.46 (m, 16H, P*Ph*), 7.51-7.58 (m, 4H, P*Ph*), 9.15 (s, 1H). ^{13}C NMR (CD_3CN): δ 122.13 (q, $^{1}J_{C-F}$ = 321.3 Hz, SO_3CF_3), 127.13 (m), 128.36 (d, J_{C-P} = 30.1 Hz, PhC), 130.63 (d, J_{C-P} = 10.7 Hz, PhC), 133.02 (s, PhC), 135.27 (d, J_{C-P} = 17.4 Hz, PhC), 159.19 (t, $^{1}J_{C-P}$ = 16.4 Hz, pyrimidine - *C5*), 166.43 (d, J_{C-P} = 4.69 Hz, pyrimidine – *C4*/*C6*), 170.74 (d, J_{C-P} = 43.4 Hz, pyrimidine – *C2*). ^{31}P NMR (CD_3CN): δ 10.38. ^{19}F NMR (CD_3CN): δ -79.18.

2.2 X-ray crystallography

Data collections on colorless crystals of **2, 4,** and **5** and orange crystals of **3** were undertaken by securing single crystals of each with dimensions of 0.35 x 0.27 x 0.25 mm^3 (**2**), 0.46 x 0.31 x 0.15 mm^3 (**3**), 0.57 x 0.51 x 0.43 mm^3 (**4**), and 0.27 x 0.24 x 0.19 mm^3 (**5**) respectively to Mitegen mounts using Paratone oil. All crystals had their single crystal reflection data collected using Mo $K_{\alpha 1}$ radiation (= 0.71073 Å) from a Rigaku Oxford Diffraction (ROD) SCXMini equipped with a Mercury2 CCD detector. Data for all samples were collected at 100 K. Data collection strategies to ensure completeness and desired redundancy were determined using CrystalClear [34]. Data processing for all samples was done using CrysAlis^{Pro} and included multi-scan absorption corrections applied using the SCALE3 ABSPACK scaling algorithm [35, 36]. All structures were solved via intrinsic phasing using ShelXT [37] and subjected to a least-squares refinement with ShelXL [38] within the Olex2 graphical user interface [39]. The final structural refinements included anisotropic temperature factors on all constituent non-

Table 1. X-ray crystallographic and refinement data for **2-5**.

Compound	2	3	4	5·5 CH_3CN	Compound	2	3	4	5·5 CH_3CN
CCDC code	2104157	2104158	2104159	2104160	ρ, mg/m^3	1.232	1.594	1.991	1.659
Formula	$C_{28}H_{22}N_2P_2$	$C_{31}H_{30}Cl_2I_2N_2P_2$	$C_{58}H_{44}Au_4Cl_4N_4P_4$	$C_{70}H_{59}Ag_4F_{12}N_9O_{12}P_4S_4$	μ, mm^{-1}	0.198	2.120	9.918	1.165
Formula Weight	448.41	817.21	1826.50	2129.87	Scan	ω scan	ω scan	ω scan	ω scan
Temp.	100(2)	100(2)	100(2)	100(2)	θ range, deg.	2.225 – 26.402	3.160 – 27.483	1.855 – 25.122	2.142 – 28.328
Space Group	*P2$_1$/n*	*P-1*	*P2$_1$/n*	*P1*	Reflections measured	38013	21510	52200	23625
a, Å	12.8342(5)	8.9943(10)	12.4689(6)	12.6869(7)	Ind. observed reflections	4953	7812	10833	20125
b, Å	10.7259(3)	11.4776(13)	28.7431(12)	13.1818(7)	Ind. reflections [I > 2σ]	4126	6409	8093	16082
c, Å	18.6563(7)	17.952(5)	18.0539(8)	13.8847(7)	Data/restraints/parameters	4953/145/351	7812/487/463	10883/966/866	20125/500/1220
α, deg.	90.00	75.765(5)	90.00	105.729(5)	R_{int}	0.0274	0.0466	0.0474	0.0200
β, deg.	109.702(4)	85.835(6)	109.644(5)	104.778(5)	Final R indices [I > 2σ]	R1 = 0.0360 wR2 = 0.0946	R1 = 0.0456 wR2 = 0.1138	R1 = 0.0396 wR2 = 0.0931	R1 = 0.0473 wR2 = 0.1067
γ, deg.	90.00	71.448(5)	90.00	94.708(4)	R indices (all data)	R1 = 0.0456 wR2 = 0.1016	R1 = 0.0566 wR2 = 0.1211	R1 = 0.0590 wR2 = 0.1026	R1 = 0.0670 wR2 = 0.1195
Vol. Å^3	2417.85(16)	1702.9(3)	6093.8(5)	2132.4(2)	Goodness-of-fit on F^2	1.023	1.048	1.016	1.022
Z	4	2	8	1	Flack parameter				0.04(3)

hydrogen atoms. Hydrogen atoms were attached via the riding model at calculated positions using suitable HFIX commands or in some cases located in the difference map and freely refined. As a means to achieve reasonable bond distances and thermal parameters within the structural models, combinations of the SADI, SIMU, RIGU and EADP constraints and restraints were used. A solvent mask was applied to both **4** and **5** to regions of electron density indicative of interstitial solvent molecules whose disorder could not be satisfactorily modeled. The crystallographic and refinement data for **2-5** are listed in **Table 1**. Figures illustrating the structural models as well as their respective packings were generated using Olex2.

3. Results and Discussion

3.1 Results

Compound **2** was prepared in a straightforward manner by treating 4,6-dichloropyrimidine with potassium diphenylphosphide in THF at room temperature for 12 hours. The double nucleophilic aromatic substitution of the two chlorine atoms with the two diphenylphosphino moieties was confirmed by multinuclear NMR spectroscopy and single crystal X-ray diffraction *vide infra*. With compound **2** in hand, we first interrogated the site of alkylation, e.g., the nitrogen or phosphorus atoms, by treating the diphosphine with an excess of iodomethane. Not surprisingly, exclusive alkylation of the phosphorus atoms was observed, which provided clean access to the bisphosphonium, **3**, as its iodide salt in excellent yields. Similar to compound **2**, the identity of **3** was confirmed via multinuclear NMR spectroscopy as well as single crystal X-ray diffraction.

Owing to our group's interest in unique *N*-heterocyclic carbene architectures, we were also interested in N-alkylation or arylation of compound **2** to afford appropriate precursor molecules. However, we observed that regardless of alkylating/arylating agent (including Meerwein reagents, alkyl triflates, or diaryliodonium reagents), only P-alkylation was observed, even under forcing conditions *i.e.* high temperatures, excess reagents. We also explored the potential to oxidize the phosphorus atoms in compound **2** to access a bisphosphine oxide followed by N-alkylation then reduction back to the bisphosphine, however these strategies proved to be unsuccessful as well.

Despite the inability to alkylate the nitrogen atoms in compound **2**, we next set out to explore the coordination chemistry of this potentially tetratopic bisphosphine ligand. First, 2 was treated with (tht)AuCl (tht = tetrahydrothiophene) in dichloromethane to give the desired bisdiphenylphosphino-gold(I) chloride complex 4 in excellent yield (88%). Compound **4** was a pale yellow, micro-crystalline solid which exhibited a faint emission when irradiated with a hand-held UV lamp. Emission of L-Au(I)Cl complexes is not unknown and typically arises from Au-Au aurophilic interactions in the solid state, as is the case for compound **4** (*vide infra*). Similar to compounds **2** and **3**, the gold complex **4** was also fully characterized using multinuclear NMR spectroscopy and single crystal X-ray diffraction. Unfortunately, inspection of the solid state structure of **4** indicated that although the ligand **2** has four potential Lewis basic donor sites, *i.e.* two pyrimidine nitrogen atoms and two phosphine phosphorus atoms, the nitrogen atoms did not appear to have any interaction with the gold(I) centers which were exclusively coordinated by phosphorus atoms.

In stark contrast, we found that treatment of **2** with two equivalents of silver(I) triflate (AgOTf) in acetonitrile let to formation of a silver(I) coordination polymer **5**. The polymeric nature of **5** was verified primarily single crystal X-ray diffraction. In the crystal, coordination of both pyrimidine nitrogen atoms and phosphino phosphorus atoms to silver(I) cations concomitant with a single coordinated acetonitrile molecule per silver atom observed. Gratifyingly, we were able to fully characterize this compound which illustrates that the extended polymeric network observed in the solid state persists in CD_3CN solutions of **5** (*vide infra*). Altogether, the formation of **5** and its persistence in solution demonstrated that bisphosphine **2** can serve as a tetratopic ligand.

3.2 Spectroscopic discussion

NMR spectra were recorded on Bruker Avance400 MHz/ 52mm spectrometer. Chemical shifts (δ) are given in ppm and are referenced to the residual solvent: ^{1}H: $CDCl_3$, 7.26ppm; CD_2Cl_2, 5.32 ppm; CD_3CN, 1.94 ppm; ^{13}C: $CDCl_3$, 77.0 ppm; CD_2Cl_2, 53.84 ppm; CD_3CN, 1.32 ppm; ^{31}P: H_3PO_4 0 ppm; ^{19}F: $CFCl_3$ 0 ppm. High resolution images of all NMR data can be found in the Electronic Supporting Information (ESI) for this manuscript.

All new compounds were characterized by heteronuclear NMR spectroscopy as a means to confirm their identity. For compound **2**, the ^{1}H NMR spectrum ($CDCl_3$) exhibited two salient signals with both integrated top 1 proton, a triplet centered at 6.69 ppm ($^2J_{H\text{-}P}$ = 0.46 Hz) corresponding the C5-*H* nucleus and a doublet centered at 9.20 ppm ($^4J_{H\text{-}P}$ = 0.60 Hz) corresponding to the C2-*H* nucleus. The only other signal observed in the ^{1}H NMR spectrum of **2** as a large multiplet centered at 7.32 ppm which integrated to 20 protons corresponding to the four phenyl rings on the two diphenylphosphino moieties. The ^{31}P NMR spectrum of **2** ($CDCl_3$) was also consistent with a molecule containing a diphenylphosphino arene with a single resonance observed at -3.12 ppm. Upon methylation of compound **2** with iodomethane to give the bisphosphonium salt **3**, two key spectroscopic changes were observed in the ^{1}H and ^{31}P NMR spectra ($CDCl_3$). First, in the ^{1}H NMR spectrum of the appearance of a doublet centered at 3.42 ppm ($^2J_{H\text{-}P}$ = 13.92 Hz) which integrated to 6 protons was observed, and second, there was a single peak observed in the ^{31}P NMR at 19.3 ppm. Both observations were fully consistent with alkylation of both phosphorus atoms in compound **2** to give the dication **3** which contained two chemically shift equivalent methyl-diphenylphosphonium moieties. Further evidence of the dicationic nature of **3** could be observed in the ^{1}H NMR spectrum which also exhibited very downfield signals corresponding to the C2-*H* and C5-*H* nuclei at 9.55 and 9.05 ppm, respectively.

The two metal complexes **4** and **5** were also characterized using multinuclear NMR spectroscopy. For the gold(I) complex **4**, the ^{1}H NMR spectrum (CD_2Cl_2) exhibited a signature downfield signal at 9.42 ppm which corresponded to the C2-*H* proton. Unlike compounds **2** and **3**, the C5-*H* resonance was not well-isolated from the diphenylphosphino aromatic protons, and could therefore not be conclusively identified. The ^{31}P NMR spectrum of complex 4 exhibited a single resonance at 33.32 ppm, was also consistent with previously reported triarylphosphino-Au(I)X (X = Cl, OTf, NTf_2, etc.) complexes (range: 29.9–32.7 ppm, *i.e.* Ph3P→AuCl ^{31}P chemical shift is 32.7 ppm in CD_2Cl_2).[40] As described in the previous section, complex **4** also exhibited a faint blue-green emission in both solution and the solid state. To this end an emission spectrum was obtained on solid powder of **4**. The emission spectrum of 4 exhibited an emission band centered at λ_{max} = 530 nm (λ_{ex} = 480 nm), consistent with the color observed by the naked eye. As described in the next section, we believe that this emission likely originates from Au–Au aurophilic interactions which were observed in the solid state structure of **4**.

Finally, the silver coordination polymer, compound **5**, exhibited a similar ^{1}H NMR spectrum (CD_3CN) to the free bisphosphine **2** with the C2-*H* and C5-*H* signals appearing at 9.15 and 6.32, respectively. However, we also observed a singlet centered at 2.23 ppm which integrated to 6 protons. Based on the single crystal X-ray diffraction data (vide infra), we believe this signal corresponds to the two coordinated acetonitrile molecules (one CH_3CN per Ag(I) cation) observed in the solid state structure. As described below, there are two Ag(I) cations coordinated by a single ligand **2**, and therefore the coordination polymer persists in solution, as evidenced by the two molecules of coordinated acetonitrile per one molecule of ligand **2** observed in the ^{1}H NMR spectrum. per one molecule of ligand 2. In agreement with this assessment, the ^{31}P NMR spectrum (CD_3CN) which revealed on a single resonance centered at 10.30 ppm was also consistent with the formation of triarylphosphino silver(I) triflate complexes, *i.e.* range of ^{31}P NMR resonances for Ph_3P→Ag(I)OTf: 10.05–15.23 ppm in CD_2Cl_2 and solid state.[41, 42]

Recently, Artem'ev and coworkers reported Ag(I) complexes supported by diphosphine **2** with NO_3 and BF_4 counter ions which exhibited thermochromic luminescence.[31] Similar to those complexes, **5** was shown to exhibit strong luminescence which likely arises from the presence of argentophilic interactions (*vide infra*). In contrast however, there was little to no temperature dependence on the obversced emission of 5 in the solid state. Instead, a bright yellow-orange emission for 5 (λ_{max} emission =622 nm; λ_{max} excitation = 422 nm.

3.3 Structural description

The structural model for **2** crystallized in the centrosymmetric monoclinic space group $P2_1/n$ with one molecule as the contents of the asymmetric unit. Within that asymmetric unit, two of the phenyl rings demonstrated signs of positional disorder over two positions. After being split and application of suitable constraints and restraints, their occupancies were freely refined to approximate ratios of 0.54/0.46 and 0.52/0.48 with respect to one another. Given the lone pair of electrons present on the phosphorus atoms, which are linked by the pyrimidine ring which forms the linker in the bidentate phosphine, each shows distorted pyramidal coordination geometry. When one considers the orientation of one of the phenyl rings on each phosphorus atom with respect to the pyrimidine ring and the phosphorus atoms, the orientation of these forms a herringbone-like motif. The two remaining phenyl rings (one bound to each phosphorus) form a tweezer-like motif with a centroid-to-centroid separation distance between the rings of 4.407(15) Å. Additionally, the angle for the tweezer-like motif measured using the centroids of the phenyl rings and C14 on the pyrimidine ligand is 69.38(3)°. Extended packing along the *b*-axis suggests that additional structural stability is provided by electron donation from the lone pair of electrons on phosphorus atom P2 to the electron-deficient center of the aromatic pyrimidine ring as evidenced by their being superimposed upon one another at distance of 3.99(4) Å. An aniostropic displacement ellipsoid plot of **2** with ellipsoids set to the 50% probability level as well as a packing representation of the molecule in the crystallographic *ac*-plane are shown in Figures **1** and **2**.

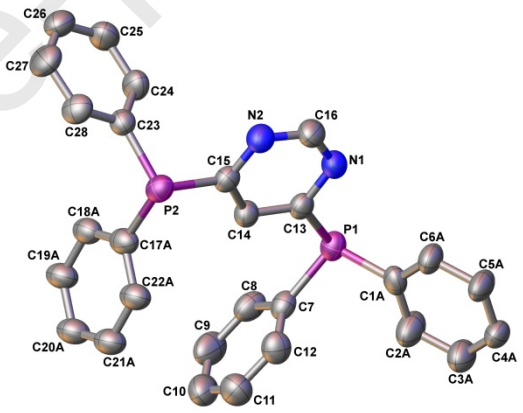

Figure 1. Anisotropic displacement ellipsoid plot of **2** with ellipsoids set to the 50% probability level. Hydrogen atoms and secondary conformations of disordered phenyl rings were omitted for clarity.

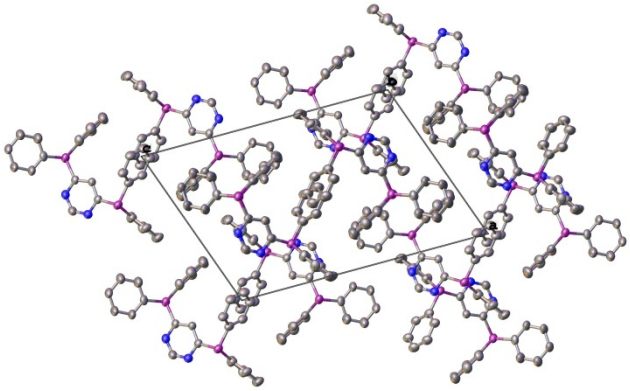

Figure 2. Packing projection of **2** in the *ac*-plane with anisotropic displacement ellipsoids set to 50% probability. Hydrogen atoms and secondary conformations of disordered phenyl rings were omitted for clarity.

The diphosphonium salt (**3**) crystallized in the centrosymmetric triclinic space group *P-1* with one dication, two iodide counterions, and one interstitial molecule of CH_2Cl_2 as the contents of the asymmetric unit. All four phenyl rings as well as the CH_2Cl_2 solvent molecule were disordered over two positions with occupancy ratios freely-refined to 0.54/0.46, 0.55/0.45, 0.62/0.38, and 0.72/0.28 respectively.. Coordination of the methyl groups to each of the phosphorus atoms forces the coordination environment around each of those atoms to become a distorted tetrahedron. Like **2**, a herringbone-like motif involving a phenyl ring on each phosphorus and the pyrimidine ring separating those phosphorus atoms forms within the structure of **3**. Analogous to **2**, the two remaining phenyl rings within **3** also form a tweezer-like motif with a centroid-to-centroid separation distance between the rings of 4.5915(15) Å and an angle measured using the centroids of the phenyl rings and C15 on the pyrimidine ligand of 70.59(6)°. The two iodide anions needed to balance the charge from the diphosphonium dication, while lying above and below the plane of pyrimidine ring, do not directly superimpose over the centroid of that ring. An aniostropic displacement ellipsoid plot of **3** with ellipsoids set to the 50% probability level as well as a packing representation of the molecule in the crystallographic *bc*-plane are shown in Figures **3** and **4**.

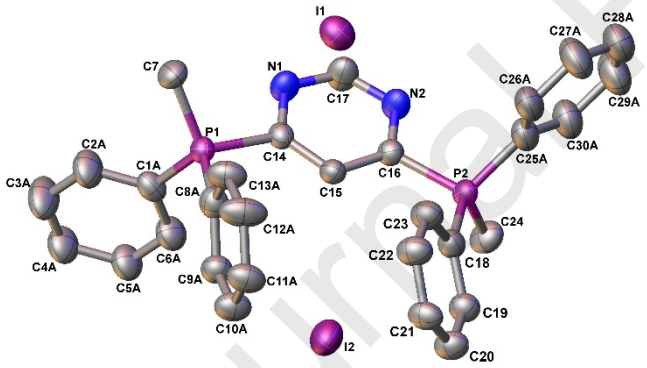

Figure 3. Anisotropic displacement ellipsoid plot of **3** with ellipsoids set to the 50% probability level. Hydrogen atoms, secondary conformations of disordered phenyl rings within the dication, and the disordered, interstitial CH_2Cl_2 were omitted for clarity.

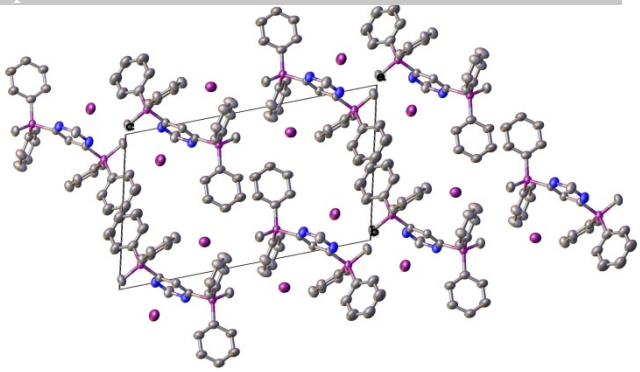

Figure 4. Packing projection of **3** in the *bc*-plane with anisotropic displacement ellipsoids set to 50% probability. Hydrogen atoms, secondary conformations of disordered phenyl rings within the dication, and disordered, interstitial CH_2Cl_2 molecules were omitted for clarity.

The gold coordination polymer (**4**) crystallized in the centrosymmetric monoclinic space group $P2_1/n$ with two molecules of phosphine **2** each bridging two Au(I) cations whose charge is balanced by terminal chlorides as the contents of the asymmetric unit. Seven of the eight phenyl rings from the two phosphine molecules in the asymmetric unit show are disordered over two positions with occupancy ratios freely-refined to 0.61/0.39 (x2), 0.58/0.42, 0.52/0.48, 0.54/0.46, 0.71/0.29, and 0.53/0.47. With the coordination of the gold atoms, each phosphorus atom adopts near-tetrahedral coordination geometry while the terminal gold atoms at the end of the asymmetric unit demonstrate linear geometry. In the center of the asymmetric unit, the two neighboring gold atoms are linked by an aurophilic interaction of 3.0626(5) Å (range for aurophilic interactions: 2.75 Å– 3.50 Å; [43, 44] sum of Au van der Waals radii = 3.60Å[45]) which causes Au2 and Au3 to have a T-shaped geometry. Along the *n*-glide, the asymmetric unit orients itself in a right-handed helical orientation with a turn between another set of symmetry-equivalent gold diphosphine helices stabilized by weak aurophilic contacts of 3.4210(5) Å between Au1 and Au4. Analogous to **2** and **3**, diphenyl tweezers were also observed with centroid-to-centroid separation distances between the rings of 4.4211(2) and 4.5221(2) Å and the measured angles of the phenyl centroid to pyrimidine carbon atoms were 69.49(14)° and 71.73(13) ° for compound **4**. An aniostropic displacement ellipsoid plot of **4** with ellipsoids set to the 50% probability level as well as a packing representation of the molecule demonstrating the helices along the *n*-glide are shown in Figures **5** and **6**.

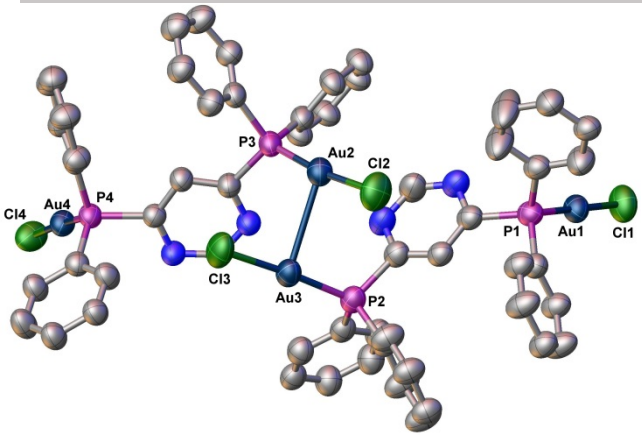

Figure 5. Anisotropic displacement ellipsoid plot of **4** with ellipsoids set to the 50% probability level. Hydrogen atoms and secondary conformations of disordered phenyl rings were omitted for clarity.

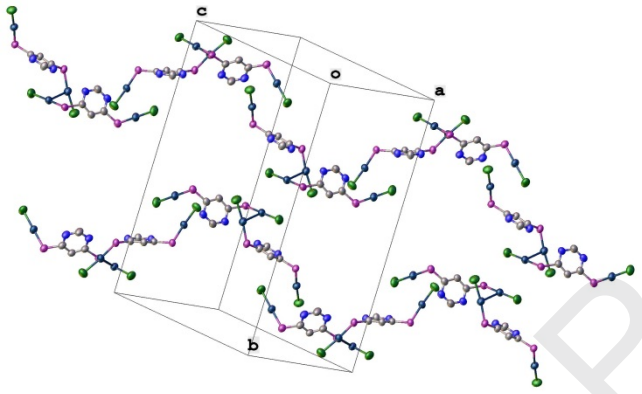

Figure 6. Projection of the helices within **4** along the *n*-glide with ellipsoids set to the 50% probability level. Hydrogen atoms and phenyl rings were omitted for clarity.

The silver coordination polymer (**5**) crystallized in the non-centrosymmetric triclinic space group *P1* and encompassed two molecules of phosphine **2**, four Ag(I) atoms, four triflate anions, and both coordinated and free CH_3CN molecules as the contents of its asymmetric unit. For the incorporated phosphine molecules, both the phosphorus atoms and pyrimidine nitrogen atoms from the central aromatic ring coordinate in a bidentate manner to two Ag^+ cation pairs bridged by argentophilic interactions of 3.2043(10) (Ag2–Ag3) and 3.2631(9) Å (Ag1–Ag4). These observed distances are within the norm for known intermolecular argentophilic interactions (range for argentophilic interactions: 2.89 Å– 3.50 Å ; sum of Ag van der Waals radii = 3.44Å)[46] and are shorter than that observed for analogous Ag(I) complexes feature ligand **2** (Ag–Ag = 3.3352(4) Å). [31] Different coordination geometries around the Ag^+ centers, including distorted trigonal bipyramidal, distorted square pyramidal, and distorted square planar were observed. To balance the charge within the asymmetric unit, four triflate anions were included with three of them coordinated to Ag^+ centers while one remained uncoordinated. Three of the anions demonstrated evidence of disorder over two positions with occupancy ratios of 0.83/0.17, 0.77/0.23, and 0.51/0.49 between the two components. Signs of disorder were observed in three of the constituent phenyl rings within the asymmetric unit and their occupancy ratios were freely refined to 0.63/0.37, 0.53/0.47, and 0.50/0.50. Orientation of the phenyl rings from the phosphines within the asymmetric unit also show herringbone and tweezer-like motifs with centroid-to-centroid separation distances between the rings within the latter of 4.2004(3) and 4.4076(2) Å respectively. Additionally, the measured phenyl centroid to pyrimidine carbon atom angles for the tweezers were 71.58(14)° and 68.87 (13)°. Four of the five CH_3CN molecules within the asymmetric unit are coordinated to Ag^+ centers. As stated previously, a solvent mask was applied to a second uncoordinated CH_3CN molecule (6th overall) whose disorder could not be satisfactorily modeled. An anisotropic displacement ellipsoid plot of **5** with ellipsoids set to the 50% probability level as well as a figure highlighting the packing of the molecule in the *ab*-plane are shown in Figures **7** and **8**.

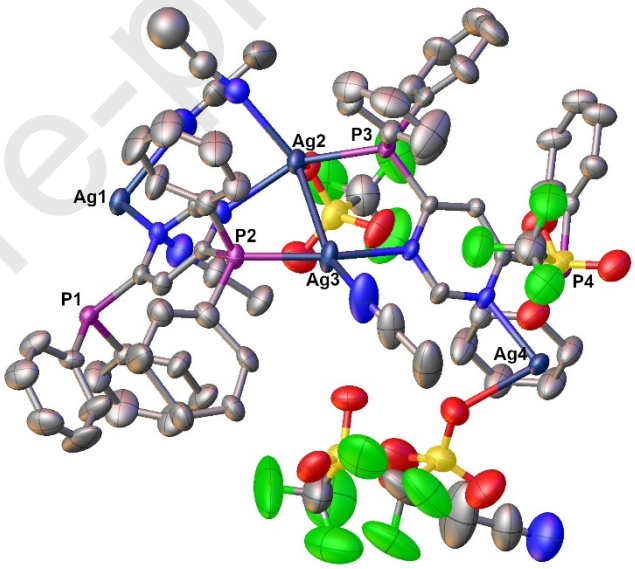

Figure 7. Anisotropic displacement ellipsoid plot of **5** with ellipsoids set to the 50% probability level. Hydrogen atoms, secondary conformations of disordered phenyl rings and triflate anions, and the free, interstitial CH_3CN molecule located in the difference map were omitted for clarity.

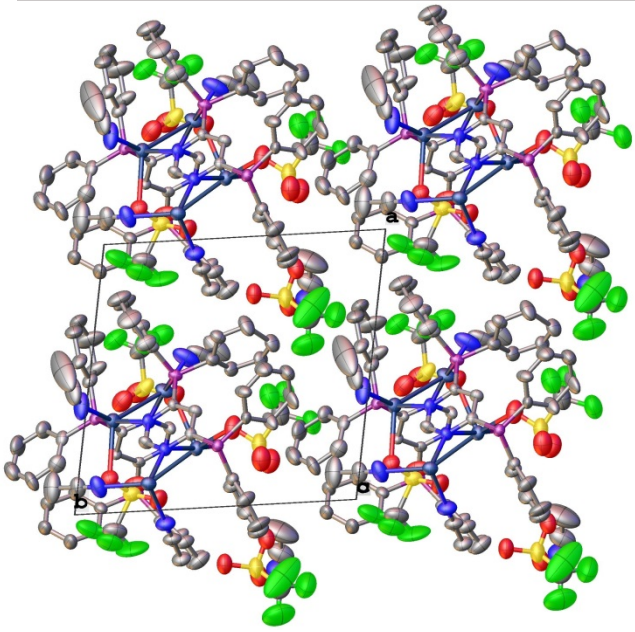

Figure 8. Packing projection of **5** in the *ab*-plane with anisotropic displacement ellipsoids set to 50% probability. Hydrogen atoms, secondary conformations of disordered phenyl rings and triflate anions and the interstitial CH_3CN molecule were omitted for clarity.

As previously noted, Artem'ev and co-workers reported the crystal structures of two Ag(I) complexes supported by diphosphine **2** with NO_3 and BF_4, counter ions.[31] Interestingly, the former crystallized with a completely different arrangement of the Ag(I) cations with respect to the ligand **2**. When $AgNO_3$ was employed as the Ag(I) source, the silver cations were found to coordinate exclusively to the phosphino moieties, *i.e.* the pyrimidine nitrogen atoms did not interact with the metal. On the other hand, when 2 was treated with $AgBF_4$ in acetonitrile, the resultant complex was nearly isostructural with our silver coordination polymer **5**, but with subtle differences.

Firstly, whereas our Ag(I) complex 5, with triflate counter ions, crystallized in the triclinic space group *P1*, Artem'ev's compound, with BF_4 counter ions, crystallized in the orthorhombic $P2_12_12_1$ space group. In Artem'ev's compound, the polymer chains are built up from alternating ligand (**2**) molecules and $[Ag_2(MeCN)_3]$ units, where one silver cation is ligated to one acetonitrile molecule, and the other is ligated to two; the BF_4 counter anions are non-coordinating to the metal centers. In stark contrast, our compound **5**, which features the more coordinating triflate counter anions, the ligand bridges 4 unique, repeating silver(I) centers.

In **5**, Ag1 is coordinated by two acetonitrile molecules and makes an argentophilic interaction to Ag4 (Ag1–Ag4 = 3.2631(9) Å), and Ag4 is coordinated by two triflate counter anions. The other two unique silver cations Ag2 and Ag3 exhibit a stronger argenetophilic interaction of 3.2043(10) Å; with Ag2 coordinated by a triflate ion and an acetonitrile molecule and Ag3 coordinated by a single acetonitrile molecule. Both sets of argentophilic interactions observed in **5** were markedly shorter than that observed in Artem'ev's compound (Ag–Ag interaction of 3.3352(4) Å. This disparity is presumably due to the increased electron withdrawing ability of the coordinated triflate anions in compound **5** when compared to only acetonitrile ligands in Artem'ev's compound. Given these structural differences are subtle, yet real, they may result in the observed disparity observed when comparing the luminescent properties of **5** to its BF_4 analogue (*vide supra*).

4. Conclusions

In conclusion, we have reported the synthesis and characterization of 4,6-bis(diphenylphosphino)pyrimidine, **2**, a novel multitopic diphosphine ligand. The reaction of bisphosphine **2** with electrophiles such as iodomethane to give bisphosphonium **3**, (tht)gold(I) chloride to give complex **4**, and with silver(I) triflate to give the coordination polymer **5** was also investigated. It was found that gold complex 4 xhibited weak emission in solution and the solid state centered at λ_{max} = 530 nm owing to Au(I)··Au(I) aurophilic interactions. The preparation of novel organogold compounds continues to garner the interest of several chemists globally with many investigations into the supramolecular chemistry of gold complexes supported through aurophilic interactions.[47-50]

The formation of coordination polymer **5**, which exhibited coordination of both phosphorus and nitrogen Lewis bases in **2** to the silver(I) cations demonstrated that bisphosphine **2** may be utilized as a tetratopic ligand. Future efforts are being devoted to exploring the coordination chemistry of ligand 2 with Rh, Pt, and Pd which may lead to unique catalysts in their own right. We are also actively exploring the chemistry of bisphosphonium **3**.

ASSOCIATED CONTENT

Supporting Information. An electronic supporting information file which contains the multinuclear NMR spectral data for all compounds as well as the emission spectrum of compound **4** are provided. Crystallographic information files (CIFs) 2104157, 2104158, 2104159, and 2104160 for compounds **2**-**5**, respectively are also available through the Cambridge Crystallographic Data Centre (CCDC) at https://www.ccdc.cam.ac.uk/.

AUTHOR INFORMATION

Corresponding Author

* Corresponding author Prof. Todd W. Hudnall, Department of Chemistry and Biochemistry, Texas State University, San Marcos, TX 78666, USA. Email: hudnall@txstate.edu

Present Addresses

†Roberta Rodrigues, Molecular Catalysis Team, Pacific Northwest National Laboratory, PO Box 999, MSIN: K2-57, Richland, WA 99352, USA.

Author Contributions

The manuscript was written through contributions of all authors.

ACKNOWLEDGMENT

The authors would like to thank the National Science Foundation grant CHE-1955396 and the Robert A. Welch Foundation (AI-1993-20190330) for generous financial support.

REFERENCES

[1] R. Saha, B. Mondal, P.S. Mukherjee, Chem. Rev., (2022).
[2] Q. He, G.I. Vargas-Zúñiga, S.H. Kim, S.K. Kim, J.L. Sessler, Chem. Rev., 119 (2019) 9753-9835.
[3] S. Durot, J. Taesch, V. Heitz, Chem. Rev., 114 (2014) 8542-8578.
[4] M. Gutiérrez, Y. Zhang, J.-C. Tan, Chem. Rev., (2022).
[5] Y. Liu, K. Ye, Y. Wang, Q. Zhang, X. Bu, P. Feng, Dalton Transactions, 46 (2017) 1481-1486.
[6] L. Rocchigiani, M. Bochmann, Chem. Rev., 121 (2021) 8364-8451.
[7] A.J. Boydston, K.A. Williams, C.W. Bielawski, J. Am. Chem. Soc., 127 (2005) 12496-12497.
[8] D.M. Khramov, A.J. Boydston, C.W. Bielawski, Angew. Chem. Int. Ed., 45 (2006) 6186-6189.
[9] H.-U. Blaser, W. Brieden, B. Pugin, F. Spindler, M. Studer, A. Togni, Topics in Catalysis, 19 (2002) 3-16.
[10] T.T.L. Au-Yeung, A.S.C. Chan, Coord. Chem. Rev., 248 (2004) 2151-2164.
[11] E.S. Wiedner, A.M. Appel, S. Raugei, W.J. Shaw, R.M. Bullock, Chem. Rev., (2022).
[12] C.A. Bessel, P. Aggarwal, A.C. Marschilok, K.J. Takeuchi, Chem. Rev., 101 (2001) 1031-1066.
[13] N.A. Eberhardt, H. Guan, Chem. Rev., 116 (2016) 8373-8426.
[14] N. Mirzadeh, T.S. Reddy, S.K. Bhargava, Coord. Chem. Rev., 388 (2019) 343-359.
[15] Y. Wang, M. Liu, R. Cao, W. Zhang, M. Yin, X. Xiao, Q. Liu, N. Huang, Journal of Medicinal Chemistry, 56 (2013) 1455-1466.
[16] Y. Zhang, M. Schulz, M. Wächtler, M. Karnahl, B. Dietzek, Coord. Chem. Rev., 356 (2018) 127-146.
[17] B. Michelet, C. Deldaele, S. Kajouj, C. Moucheron, G. Evano, Organic Letters, 19 (2017) 3576-3579.
[18] J. Fajardo, J.C. Peters, Inorg. Chem., 60 (2021) 1220-1227.
[19] R. Langer, G. Leitus, Y. Ben-David, D. Milstein, Angew. Chem. Int. Ed., 50 (2011) 2120-2124.
[20] D.V. Gutsulyak, W.E. Piers, J. Borau-Garcia, M. Parvez, J. Am. Chem. Soc., 135 (2013) 11776-11779.
[21] A.M. Poitras, S.E. Knight, M.W. Bezpalko, B.M. Foxman, C.M. Thomas, Angew. Chem. Int. Ed., 57 (2018) 1497-1500.
[22] W.H. Bernskoetter, C.K. Schauer, K.I. Goldberg, M. Brookhart, Science, 326 (2009) 553-556.
[23] T.-P. Lin, J.C. Peters, J. Am. Chem. Soc., 135 (2013) 15310-15313.
[24] H. Yang, F.P. Gabbaï, J. Am. Chem. Soc., 136 (2014) 10866-10869.
[25] S. Sahu, F.P. Gabbaï, J. Am. Chem. Soc., 139 (2017) 5035-5038.
[26] Q. Lai, M.N. Cosio, O.V. Ozerov, Chem. Commun., 56 (2020) 14845-14848.
[27] Q. Lai, N. Bhuvanesh, O.V. Ozerov, J. Am. Chem. Soc., 142 (2020) 20920-20923.
[28] S.A. Burgess, A. Kassie, S.A. Baranowski, K.J. Fritzsching, K. Schmidt-Rohr, C.M. Brown, C.R. Wade, J. Am. Chem. Soc., 138 (2016) 1780-1783.
[29] R.E. Sikma, P. Kunal, S.G. Dunning, J.E. Reynolds, J.S. Lee, J.-S. Chang, S.M. Humphrey, J. Am. Chem. Soc., 140 (2018) 9806-9809.
[30] H.-H. Cui, N.-N. Wu, J.-Y. Wang, M.-Q. Hu, H.-M. Wen, C.-N. Chen, Journal of Organometallic Chemistry, 767 (2014) 46-53.
[31] A.V. Artem'ev, M.P. Davydova, A.S. Berezin, D.G. Samsonenko, Inorganics, 8 (2020) 46.
[32] E.M. Hanawalt, J. Farkas, H.G. Richey, Organometallics, 23 (2004) 416-422.
[33] Y. Tsuchido, R. Abe, T. Ide, K. Osakada, Angew. Chem. Int. Ed., 59 (2020) 22928-22932.
[34] CrystalClear, Rigaku Corporation, version 2.0r15, 2008
[35] CrysAlisPro, Rigaku Oxford Diffraction, 171.39.27b, 2017
[36] SCALE3 ABSPACK - A Rigaku Oxford Diffraction program for Absorption Correction, Rigaku Oxford Diffraction, 2017
[37] G. Sheldrick, Acta Crystallogr. A, 71 (2015) 3-8.
[38] G.M. Sheldrick, Acta Crystallogr. C, 71 (2015) 3-8.
[39] O.V. Dolomanov, L.J. Bourhis, R.J. Gildea, J.A.K. Howard, H. Puschmann, J. Appl. Cryst., 42 (2009) 339-341.
[40] R.E.M. Brooner, T.J. Brown, R.A. Widenhoefer, Chem. Eur. J., 19 (2013) 8276-8284.
[41] L. Lettko, J.S. Wood*, M.D. Rausch*, Inorganica Chimica Acta, 308 (2000) 37-44.
[42] P. Miller, M. Nieuwenhuyzen, J.P.H. Charmant, S.L. James, CrystEngComm, 6 (2004) 408-412.
[43] N. Mirzadeh, S.H. Privér, A.J. Blake, H. Schmidbaur, S.K. Bhargava, Chem. Rev., 120 (2020) 7551-7591.
[44] H. Schmidbaur, A. Schier, Chemical Society Reviews, 37 (2008) 1931-1951.
[45] D. Blasco, J.M. López-de-Luzuriaga, M. Monge, M.E. Olmos, M. Rodríguez-Castillo, H. Amaveda, M. Mora, V. García Sakai, J.A. Martínez-González, Inorganic Chemistry Frontiers, 8 (2021) 3707-3715.
[46] H. Schmidbaur, A. Schier, Angew. Chem. Int. Ed., 54 (2015) 746-784.
[47] S. Ibáñez, M. Poyatos, E. Peris, Acc. Chem. Res., 53 (2020) 1401-1413.
[48] Y.-F. Hsu, T.-W. Wu, Y.-H. Kang, C.-Y. Wu, Y.-H. Liu, S.-M. Peng, K.V. Kong, J.-S. Yang, Inorg. Chem., 61 (2022) 11981-11991.
[49] J. Gil-Rubio, J. Vicente, Chem. Eur. J., 24 (2018) 32-46.
[50] P. Shang, Y. Wu, Z.-H. Jiang, H.-Z. He, Q. Huang, X.-Q. Pu, Y.-Q. Xiao, X.-F. Jiang, Inorg. Chem., (2022) ASAP Article.

[1] R. Saha, B. Mondal, P.S. Mukherjee, Chem. Rev., (2022).
[2] Q. He, G.I. Vargas-Zúñiga, S.H. Kim, S.K. Kim, J.L. Sessler, Chem. Rev., 119 (2019) 9753-9835.
[3] S. Durot, J. Taesch, V. Heitz, Chem. Rev., 114 (2014) 8542-8578.
[4] M. Gutiérrez, Y. Zhang, J.-C. Tan, Chem. Rev., (2022).
[5] Y. Liu, K. Ye, Y. Wang, Q. Zhang, X. Bu, P. Feng, Dalton Transactions, 46 (2017) 1481-1486.
[6] L. Rocchigiani, M. Bochmann, Chem. Rev., 121 (2021) 8364-8451.
[7] A.J. Boydston, K.A. Williams, C.W. Bielawski, J. Am. Chem. Soc., 127 (2005) 12496-12497.
[8] D.M. Khramov, A.J. Boydston, C.W. Bielawski, Angew. Chem. Int. Ed., 45 (2006) 6186-6189.
[9] H.-U. Blaser, W. Brieden, B. Pugin, F. Spindler, M. Studer, A. Togni, Topics in Catalysis, 19 (2002) 3-16.
[10] T.T.L. Au-Yeung, A.S.C. Chan, Coord. Chem. Rev., 248 (2004) 2151-2164.
[11] E.S. Wiedner, A.M. Appel, S. Raugei, W.J. Shaw, R.M. Bullock, Chem. Rev., (2022).
[12] C.A. Bessel, P. Aggarwal, A.C. Marschilok, K.J. Takeuchi, Chem. Rev., 101 (2001) 1031-1066.
[13] N.A. Eberhardt, H. Guan, Chem. Rev., 116 (2016) 8373-8426.
[14] N. Mirzadeh, T.S. Reddy, S.K. Bhargava, Coord. Chem. Rev., 388 (2019) 343-359.
[15] Y. Wang, M. Liu, R. Cao, W. Zhang, M. Yin, X. Xiao, Q. Liu, N. Huang, Journal of Medicinal Chemistry, 56 (2013) 1455-1466.
[16] Y. Zhang, M. Schulz, M. Wächtler, M. Karnahl, B. Dietzek, Coord. Chem. Rev., 356 (2018) 127-146.
[17] B. Michelet, C. Deldaele, S. Kajouj, C. Moucheron, G. Evano, Organic Letters, 19 (2017) 3576-3579.
[18] J. Fajardo, J.C. Peters, Inorg. Chem., 60 (2021) 1220-1227.
[19] R. Langer, G. Leitus, Y. Ben-David, D. Milstein, Angew. Chem. Int. Ed., 50 (2011) 2120-2124.
[20] D.V. Gutsulyak, W.E. Piers, J. Borau-Garcia, M. Parvez, J. Am. Chem. Soc., 135 (2013) 11776-11779.
[21] A.M. Poitras, S.E. Knight, M.W. Bezpalko, B.M. Foxman, C.M. Thomas, Angew. Chem. Int. Ed., 57 (2018) 1497-1500.
[22] W.H. Bernskoetter, C.K. Schauer, K.I. Goldberg, M. Brookhart, Science, 326 (2009) 553-556.
[23] T.-P. Lin, J.C. Peters, J. Am. Chem. Soc., 135 (2013) 15310-15313.
[24] H. Yang, F.P. Gabbaï, J. Am. Chem. Soc., 136 (2014) 10866-10869.
[25] S. Sahu, F.P. Gabbaï, J. Am. Chem. Soc., 139 (2017) 5035-5038.
[26] Q. Lai, M.N. Cosio, O.V. Ozerov, Chem. Commun., 56 (2020) 14845-14848.
[27] Q. Lai, N. Bhuvanesh, O.V. Ozerov, J. Am. Chem. Soc., 142 (2020) 20920-20923.
[28] S.A. Burgess, A. Kassie, S.A. Baranowski, K.J. Fritzsching, K. Schmidt-Rohr, C.M. Brown, C.R. Wade, J. Am. Chem. Soc., 138 (2016) 1780-1783.
[29] R.E. Sikma, P. Kunal, S.G. Dunning, J.E. Reynolds, J.S. Lee, J.-S. Chang, S.M. Humphrey, J. Am. Chem. Soc., 140 (2018) 9806-9809.
[30] H.-H. Cui, N.-N. Wu, J.-Y. Wang, M.-Q. Hu, H.-M. Wen, C.-N. Chen, Journal of Organometallic Chemistry, 767 (2014) 46-53.
[31] A.V. Artem'ev, M.P. Davydova, A.S. Berezin, D.G. Samsonenko, Inorganics, 8 (2020) 46.
[32] E.M. Hanawalt, J. Farkas, H.G. Richey, Organometallics, 23 (2004) 416-422.
[33] Y. Tsuchido, R. Abe, T. Ide, K. Osakada, Angew. Chem. Int. Ed., 59 (2020) 22928-22932.
[34] CrystalClear, Rigaku Corporation, version 2.0r15, 2008
[35] CrysAlisPro, Rigaku Oxford Diffraction, 171.39.27b, 2017
[36] SCALE3 ABSPACK - A Rigaku Oxford Diffraction program for Absorption Correction, Rigaku Oxford Diffraction, 2017
[37] G. Sheldrick, Acta Crystallogr. A, 71 (2015) 3-8.
[38] G.M. Sheldrick, Acta Crystallogr. C, 71 (2015) 3-8.

[39] O.V. Dolomanov, L.J. Bourhis, R.J. Gildea, J.A.K. Howard, H. Puschmann, J. Appl. Cryst., 42 (2009) 339-341.
[40] R.E.M. Brooner, T.J. Brown, R.A. Widenhoefer, Chem. Eur. J., 19 (2013) 8276-8284.
[41] L. Lettko, J.S. Wood*, M.D. Rausch*, Inorganica Chimica Acta, 308 (2000) 37-44.
[42] P. Miller, M. Nieuwenhuyzen, J.P.H. Charmant, S.L. James, CrystEngComm, 6 (2004) 408-412.
[43] N. Mirzadeh, S.H. Privér, A.J. Blake, H. Schmidbaur, S.K. Bhargava, Chem. Rev., 120 (2020) 7551-7591.
[44] H. Schmidbaur, A. Schier, Chemical Society Reviews, 37 (2008) 1931-1951.
[45] D. Blasco, J.M. López-de-Luzuriaga, M. Monge, M.E. Olmos, M. Rodríguez-Castillo, H. Amaveda, M. Mora, V. García Sakai, J.A. Martínez-González, Inorganic Chemistry Frontiers, 8 (2021) 3707-3715.
[46] H. Schmidbaur, A. Schier, Angew. Chem. Int. Ed., 54 (2015) 746-784.
[47] S. Ibáñez, M. Poyatos, E. Peris, Acc. Chem. Res., 53 (2020) 1401-1413.
[48] Y.-F. Hsu, T.-W. Wu, Y.-H. Kang, C.-Y. Wu, Y.-H. Liu, S.-M. Peng, K.V. Kong, J.-S. Yang, Inorg. Chem., 61 (2022) 11981-11991.
[49] J. Gil-Rubio, J. Vicente, Chem. Eur. J., 24 (2018) 32-46.
[50] P. Shang, Y. Wu, Z.-H. Jiang, H.-Z. He, Q. Huang, X.-Q. Pu, Y.-Q. Xiao, X.-F. Jiang, Inorg. Chem., (2022) ASAP Article.